

# Two-Dimensional Direction in The Neural Networks with Radial Basis Function

Marija Agatonovic<sup>1</sup>, Zoran Stankovic<sup>1</sup>, Bratislav Milovanovic<sup>1</sup>, Ivan Milovanovic<sup>2</sup> and Nebojsa Doncov<sup>1</sup>

<sup>1</sup>University of Nis

Aleksandra Medvedeva 14

18000 Nis, Serbia

[marija.agatonovic@elfak.ni.ac.rs](mailto:marija.agatonovic@elfak.ni.ac.rs)

<sup>2</sup>Singidunum University

Danijelova 29-32

11000 Belgrade, Serbia



**ABSTRACT:** *We have used the two-dimensional direction of arrival for calculating the coherent sources with the application of radial basis function. We further used the narrowband signals and rectangular antenna array geometry for network training. The experimental set up and finding is carried out to find the efficiency in the 2D estimation that ultimately help to separate the closely space coherent sources. The RBF neural network paves the way for operating the real-time representation using algorithms.*

**Keywords:** Coherent Sources, Direction of Arrival Estimation, Radial Basis Function (RBF) Neural Network, Rectangular Antenna Array

**Received:** 1 July 2022, Revised 4 October 2022, Accepted 20 October 2022

**DOI:** 10.6025/jnt/2022/13/4/91-98

**Copyright:** with Authors

## 1. Introduction

Smart antenna plays crucial role in modern wireless communication systems. By adjusting the beam pattern as the desired user and interference move it is able to significantly improve the system capacity. Concerning this, direction-ofarrival (DOA) estimation of users' signals is performed using the spatial covariance matrix of received signals at antenna array elements. Based on the information provided by the DOA estimation algorithm, weights are calculated and radiation pattern of the array is reshaped to amplify the desired signal and cancel the interference. To estimate DOAs of non-coherent sources the subspace based methods reported in [1] and [2] use the property that the rank of the signal component of a nonsingular spatial covariance matrix equals the number of radiating sources. In this case, the signal and noise subspaces can be obtained by eigen-decomposition of the covariance matrix. However, this property is not valid for coherent sources. The spatial smoothing is the best known preprocessing technique that is applied to circumvent the problems encountered in DOA estimation of coherent signals [3]. A disadvantage of spatial smoothing is the requirement to form subarrays whose number must be equal to or greater than the number of signals. This effectively reduces the antenna array size and ultimately reduces the resolution of the estimation method. Therefore, this technique has shortcomings when DOAs of closely spaced coherent sources have to be estimated.

In this paper, we propose a RBF neural network-based model to estimate DOAs of coherent sources in both azimuth and

elevation. As shown in the paper, this approach is very efficient and accurate as it is independent on the eigenstructure of the covariance matrix [4]. DOA estimation is based on the simulation data of two coherent sources at the same elevation and different azimuth angles and mutual distances. The observed space is from  $-45^\circ$  to  $45^\circ$ , both in azimuth and elevation plane. Performance of the developed neural model is verified using test data, not included in the training process. The obtained results and comparison to MUSIC with SSP proves the good generalization capability of the RBF neural model.

This paper is organized as follows. Section 2 introduces the signal model for narrowband coherent sources. Section 3 describes the architecture of an RBF neural network (RBFNN) and corresponding training procedure. Section 4 presents data pre-processing for the network training, RBFNN modeling results and comparison with MUSIC with SSP. Section 6, the Conclusion, summarizes the main results.

## 2. Signal Model

Let us consider a uniform rectangular array (URA) composed of  $M \times N$  omnidirectional antenna elements (sensors), as shown in Fig. 1. Each antenna element is denoted by its coordinates  $(m, n)$ , where  $m = 0, 1, 2, \dots, M - 1$  and  $n = 0, 1, 2, \dots, N - 1$ . Elements of the URA are placed along the  $y$  and  $z$ -directions with constant inter-element spacing of  $dy$  and  $dz$ , respectively. To avoid spatial aliasing, distance between adjacent elements in the URA is usually half a wavelength,  $d_y = d_z = d = \lambda/2$ .

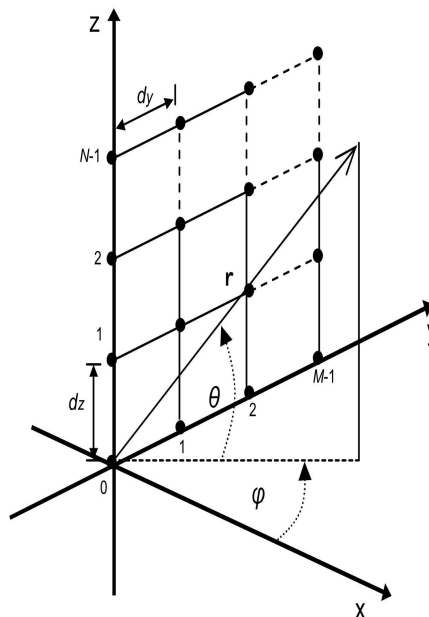


Figure 1. Uniform rectangular array (URA)

For  $K$  narrowband coherent signals, centered at frequency  $\omega_0$ , that impinge on the URA from directions  $\{(\varphi_1, \theta_1), (\varphi_2, \theta_2), \dots, (\varphi_K, \theta_K)\}$  in azimuth and elevation, the signal received by the array elements can be written as

$$\mathbf{x}(t) = \mathbf{A}(\varphi, \theta)\mathbf{s}(t) + \mathbf{n}(t) \quad (1)$$

where  $\mathbf{x}(t)$ ,  $\mathbf{n}(t)$ , and  $\mathbf{s}(t)$  are given by

$$\begin{aligned} \mathbf{x}(t) &= [x_{00}(t) \ x_{01}(t) \ \dots \ x_{0N-1}(t) \ x_{10}(t) \ x_{11}(t) \ \dots \ x_{M-1N-1}(t)]^T \\ \mathbf{n}(t) &= [n_{00}(t) \ n_{01}(t) \ \dots \ n_{0N-1}(t) \ n_{10}(t) \ n_{11}(t) \ \dots \ n_{M-1N-1}(t)]^T \\ \mathbf{s}(t) &= [s_1(t) \ s_2(t) \ \dots \ s_K(t)]^T. \end{aligned} \quad (2)$$

Vector of antenna array outputs is denoted by  $x(t)$ ,  $s(t)$  stands for the vector of source signals while  $n(t)$  represents noise vector as signals incident on the array elements are assumed to have some noise associated with them. The phase differences between signals collected by the array elements make it possible to calculate DOAs. If the phase reference point is located at  $(m, n) = (0, 0)$  then the phase of the  $k$ -th incident wave at the element with coordinates  $(m, n)$  can be written as follows

$$\phi_{m,n}^{(k)}(\varphi_k, \theta_k) = \frac{2\pi}{\lambda} (d_y m \cos\theta_k \sin\varphi_k + d_z n \sin\theta_k) \quad (3)$$

Therefore, the steering vector of the  $k$ -th incident signal is given by

$$\mathbf{a}^{(k)} = [a_{00}^{(k)} \ a_{01}^{(k)} \ \dots \ a_{0N-1}^{(k)} \ a_{10}^{(k)} \ a_{11}^{(k)} \ \dots \ a_{mn}^{(k)} \ \dots \ a_{M-1N-1}^{(k)}] \quad (4)$$

$$a_{mn}^{(k)} = a_{mn}^{(k)}(\varphi_k, \theta_k) = e^{j\phi_{m,n}^{(k)}(\varphi_k, \theta_k)}$$

where  $k = 1, 2, \dots, K$ .  $\mathbf{A}(\varphi, \theta)$  in Eq. (1) is a steering matrix whose columns are steering vectors towards  $K$  different directions of arrival and it can be written as follows

$$\mathbf{A}(\varphi, \theta) = [\mathbf{a}^{(1)} \ \mathbf{a}^{(2)} \ \mathbf{a}^{(3)} \ \dots \ \mathbf{a}^{(k)} \ \dots \ \mathbf{a}^{(K-1)} \ \mathbf{a}^{(K)}] \quad (5)$$

Finally, the spatial covariance matrix  $\mathbf{R}$  of the received noisy signals can be defined by

$$\mathbf{R} = E\{\mathbf{x}(t)\mathbf{x}^H(t)\} = \mathbf{A}\mathbf{S}\mathbf{A}^H + \sigma^2\mathbf{I} \quad (6)$$

where  $E\{\}$  is the expectation operator,  $H$  denotes the complex conjugate transpose operation,  $\sigma^2$  is the noise variance,  $\mathbf{I}$  is the identity matrix,  $\mathbf{S}$  is  $K \times K$  signal covariance matrix given by

$$\mathbf{S} = E[\mathbf{s}(t)\mathbf{s}^H(t)] = E[|s_l(t)|^2] \mathbf{c}\mathbf{c}^H \quad (7)$$

In Eq. (7),  $\mathbf{c} = [\rho_1 \ \rho_2 \ \dots \ \rho_K]^T$  where  $\rho_i$ ,  $i = 1, 2, \dots, K$ , denotes the relative amplitude and phase between the  $i$ th and  $l$ th source ( $\rho_1 = 1$ ). It can be observed that the signal subspace of matrix  $\mathbf{R}$  is of rank one instead of  $K$  and the noise subspace is orthogonal to  $\mathbf{A}\mathbf{c}$  instead of the columns of  $\mathbf{A}$  which implies the failure of the subspace based method when the spatial covariance matrix  $\mathbf{R}$  is used in this form.

### 3. Radial Basis Function (Rbf) Neural Networks

Neurons in a Radial Basis Function (RBF) neural network are organized into three layers, an input, an output as well as one hidden layer. Every neuron in each layer of the network is connected to every neuron in the adjacent forward layer, and no connections are permitted between the neurons belonging to the same layer. Each neuron is characterized by its transfer function and each connection between two neurons by a weight. Transfer functions of neurons of the input and output layers are usually linear whereas neurons of the hidden layer have radial basis transfer function that performs non-linear mapping. The main parameters of radial basis function are a centre vector and standard deviation (spread). The mapping function depends on distance between the input vector and the centre vector. An RBF network with  $n$ -dimensional input  $x \in R_n$  and  $m$ -dimensional output  $y \in R^m$  can be represented by the weighted summation of a finite number of radial basis functions as follows

$$y = F(x) = \sum_{i=1}^L w_i \psi(\|x - x_i\|) \quad (8)$$

where  $\psi(\|x-x_i\|)$  is the radial basis function of  $x$ , obtained by shifting  $\psi(\|x\|)$  by  $x_i$ .  $L$  is a set of arbitrary functions and  $x_i$  are centers of the radial basis functions. In Eq. (8),  $\psi$  is usually assumed to be un-normalized Gaussian function given by

$$\psi(x) = e^{\frac{-x^2}{2\sigma^2}} \quad (9)$$

where  $\sigma$  denotes the standard deviation of the radial basis function (spread). Gaussian function is highly nonlinear, and it is able to provide good characteristics for incremental learning.

Training process of an RBF neural network begins by separating data into training and testing set. Input and output of the network are the domain and the range pairs  $(p, t)$ , respectively. The error goal (usually MSE - Mean Squared Error) is a controlling parameter of the training process chosen in advance. In the particular case, the spread (standard deviation) of the radial basis function is equal for all hidden neurons. As the best value of this parameter cannot be a priori known, it is usually experimentally determined through the training of a number of neural networks and comparing their performance.

The algorithm used to determine the cluster centers and weights between the hidden and the output layer is Orthogonal Least Squares (OLS). Initially, the hidden layer of the network contains no neurons. Following the OLS algorithm, only one neuron is added in iteration with the center equal to the input vector that causes the maximum error. After that, weights between neurons  $(w_{i,j})$  are recalculated. This process continues until the previously defined criteria for the MSE is met or the maximum number of neurons in the hidden layer is reached.

The size of the RBF network (number of neurons in the hidden layer) is known at fully trained network. Once trained, the network is able to give accurate responses to those inputs that have not been presented to the network in the training process. The test set is taken from the same distribution as the inputs used in the training set. Accuracy of the trained RBF neural network can be expressed using statistical parameters such as worst case error (WCE (%)), average case error (ACE (%)) and Pearson Product-Moment correlation coefficient.

#### 4. Modelling Results in Case of Two Coherent Sources

The training data are collected at several positions of two coherent sources in azimuth and elevation. The observed space is from  $-45^\circ$  to  $45^\circ$ , both in azimuth and elevation. It is assumed that both sources are at the same elevation plane, and at different mutual distances in azimuth plane ( $2^\circ, 5^\circ, 10^\circ, 20^\circ, 30^\circ, 50^\circ, 60^\circ$ , and  $90^\circ$ ). The resolution of training samples is  $2^\circ$  in azimuth, and  $5^\circ$  in elevation. However, testing set is formed at mutual distances  $3^\circ, 17^\circ, 35^\circ, 55^\circ$ , and  $75^\circ$ , and in steps of  $2.7^\circ$  in azimuth and  $3^\circ$  in elevation. To simulate the presence of white Gaussian noise, random numbers were added to the training and testing data. The Signal to Noise Ratio (SNR) is assumed to be 15 dB, and distance between array elements is taken to be half a wavelength. Spatial covariance matrix is estimated from 5 snapshots of received signals.

As a first step in developing a neural network to estimate 2D DOAs, simple preprocessing of spatial covariance matrix is performed. The matrix is organized in a vector in such a manner that real and imaginary parts of complex matrix elements are separated. As the matrix  $R$  is symmetrical with respect to the diagonal, the elements of its upper triangular part provide sufficient information for DOA estimation of coherent sources. If a 16-element rectangular antenna array is employed at the receiver that implies 256 neurons in the input layer of the RBF network. Since azimuth and elevation angles of two coherent sources have to be estimated, the neural network is going to have 4 outputs (Figure 2). After a number of neural models are developed, the one demonstrating the best test statistics is chosen for 2D DOA estimation of coherent sources. In our case, the optimum RBF network contains 733 neurons in its hidden layer, and correlation coefficient of 0.9976.

The RMSE (Root Mean Squared Error) of the estimates from the testing set is plotted in Figure 3 and Figure 4 for mutual distance of  $35^\circ$  between two sources. The error is calculated using the formula

$$RMSE = \sqrt{E\{(\varphi_{ref} - \varphi_{est})^2 + (\theta_{ref} - \theta_{est})^2\}} \quad (10)$$

Keeping in mind that only one RBF neural network is employed to estimate azimuth and elevation DOAs of coherent sources,

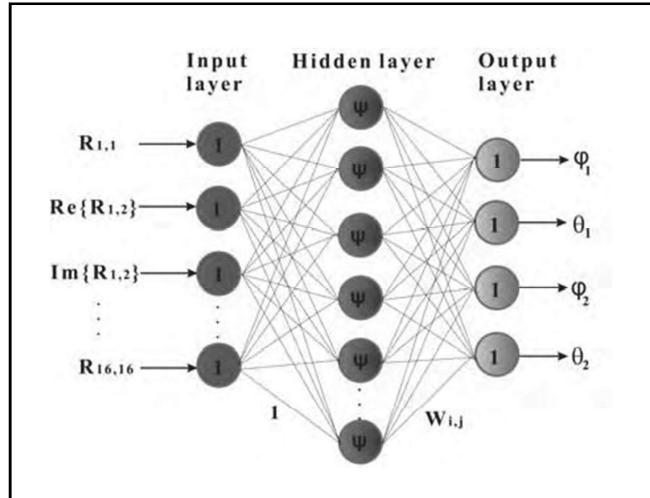


Figure 2. RBF neural model for 2D DOA estimation of coherent sources

the estimation error in Figure 3 and Figure 4 is not so significant. The network demonstrates similar performance for all incident angles of coherent signals.

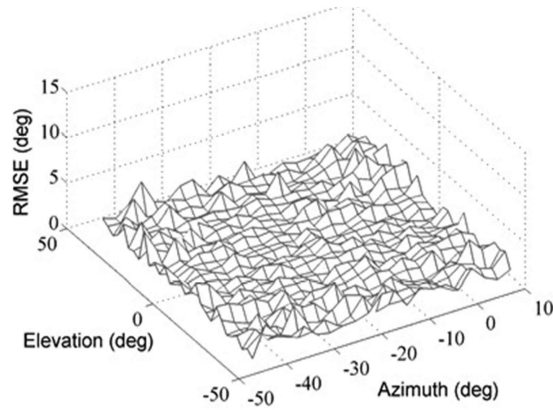


Figure 3. RMSE of the 2D DOA estimates for the first coherent source (mutual distance between sources is  $35^\circ$ )

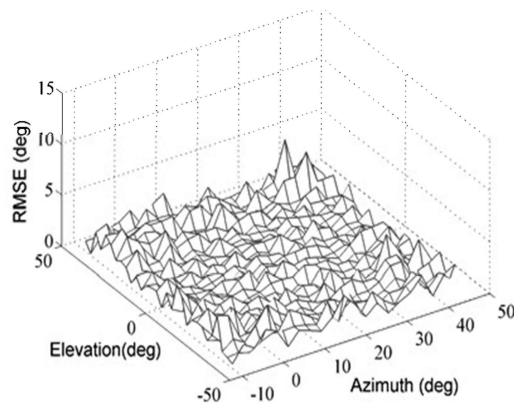


Figure 4. RMSE of the 2D DOA estimates for the second coherent source (mutual distance between sources is  $35^\circ$ )

Actual DOAs (°) ( $\varphi_1, \theta_1$ ), ( $\varphi_2, \theta_2$ ),		RBF-NN estimates (°) ( $\varphi_{1est}, \theta_{1est}$ ), ( $\varphi_{2est}, \theta_{2est}$ ),	
(-10, 10)	(10, 10)	(-9.37, 9.78)	(-9.57, 9.78)
(-14, -17)	(14, -17)	(-15.23, -16.51)	(14.43, -16.51)
(-21, 26)	(21, 26)	(-22.51, 25.69)	(22.75, 25.69)
(-30, -35)	(30, -35)	(-30.84, -35.55)	(30.60, -35.55)

Table 1. RBF-NN Estimates

Actual DOAs (°) ( $\varphi_1, \theta_1$ ), ( $\varphi_2, \theta_2$ ),		MUSIC with SSP estimates (°) ( $\varphi_{1est}, \theta_{1est}$ ), ( $\varphi_{2est}, \theta_{2est}$ )	
(-10, 10)	(10, 10)	(1, 10.5)	(1, 10.5)
(-14, -17)	(14, -17)	(8, -16.5)	(8, -16.5)
(-21, 26)	(21, 26)	(-18.5, 25)	(19.5, 26)
(-30, -35)	(30, -35)	(-31, -34.5)	(-30, -35)

Table 2. Music With Ssp Estimates

In Table 1 and Table 2, 2D DOA estimates of the RBF-NN and MUSIC algorithm with SSP are given for several positions of coherent sources. Based on this data it can be concluded that neural model gives more accurate estimates in the wide sector of azimuth and elevation angles. Further, the first two rows of the Table II show the inability of the MUSIC with SSP to separate and detect two closely spaced coherent sources.

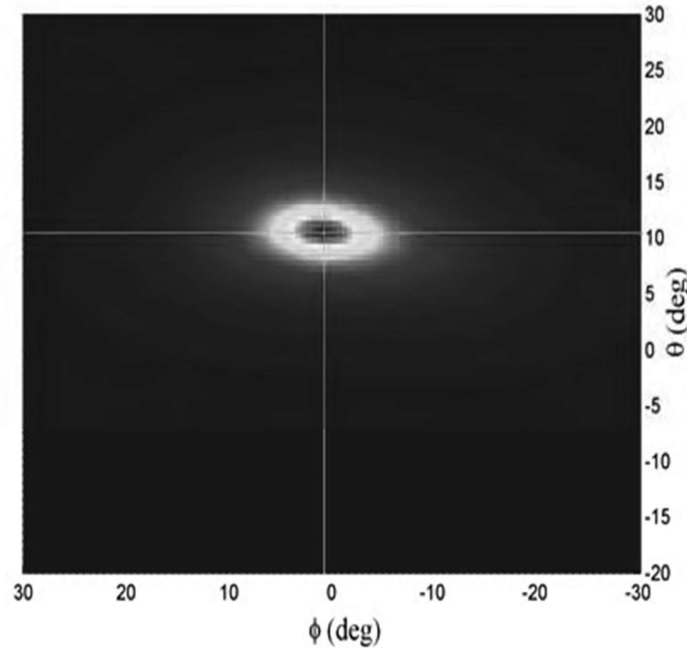


Figure 5. MUSIC with SSP spectrum for two coherent sources positioned at  $(-10^\circ, 10^\circ)$  and  $(10^\circ, 10^\circ)$

The results presented in Figure 5 and Figure 6, are consequence of a reduced effective aperture of the antenna array after the decorrelating procedure (SSP) is applied to the original spatial covariance matrix. The results can be even deteriorated in case of a lower SNR. Figure 7 demonstrates good estimation results of MUSIC, for two sources separated by  $42^\circ$ . On the other side, RBF neural network detects sources independently of their mutual distance. This feature of the network is considered as its main advantage over the conventional MUSIC with SSP. In addition, neural network considers DOA estimation as a function approxi

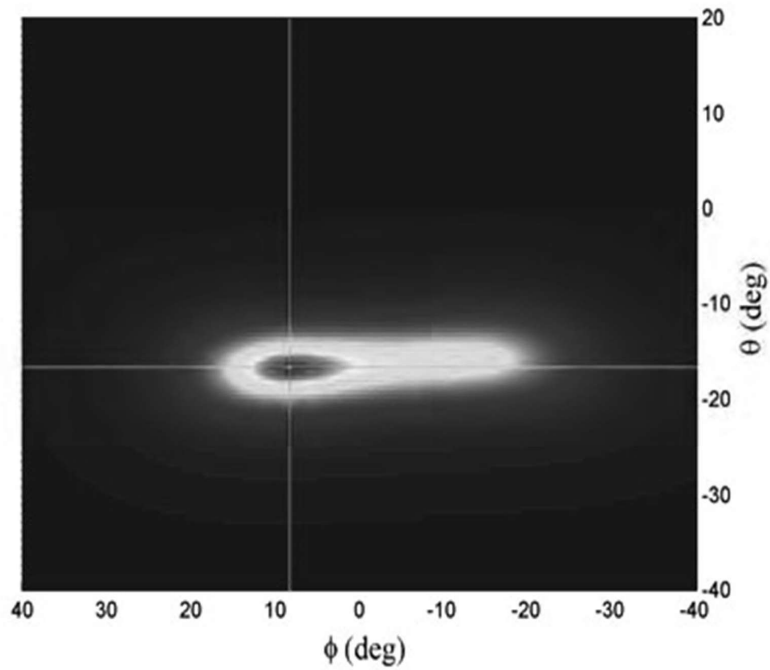


Figure 6. MUSIC with SSP spectrum for two coherent sources positioned at  $(-14^\circ, -17^\circ)$  and  $(14^\circ, -17^\circ)$

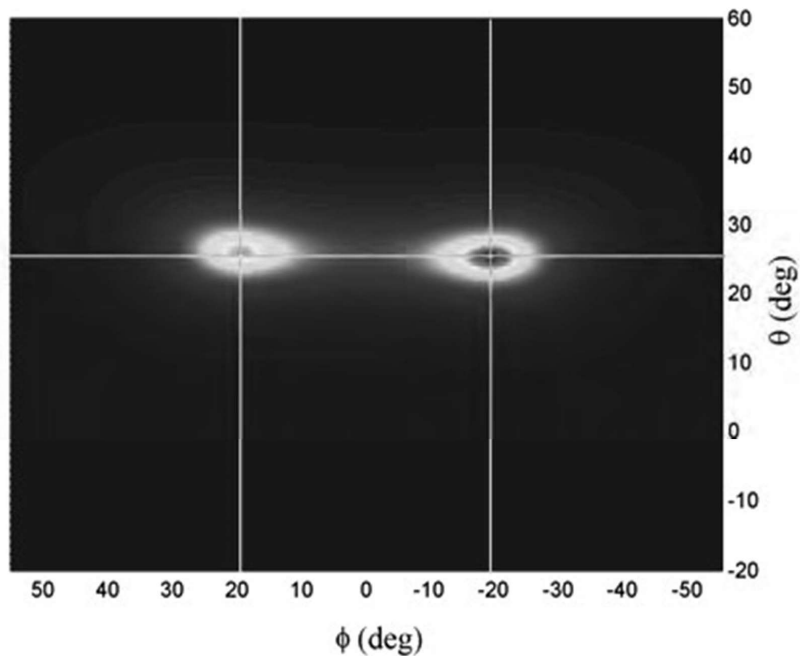


Figure 7. MUSIC with SSP spectrum for two coherent sources positioned at  $(-21^\circ, 26^\circ)$  and  $(21^\circ, 26^\circ)$

mation problem avoiding complex matrix calculations and 2D spectrum search. Therefore, it is able to obtain 2D DOA estimates in real time unlike the time-consuming MUSIC algorithm.

To improve the accuracy of RBF-NN 2D DOA estimates and to expand the observed space, authors of this work are going to develop a more complex and efficient model based on smaller RBF neural networks.

## 5. Conclusion

In this paper, we propose an RBF neural network-based model for the efficient 2D DOA estimation of coherent sources. Using the assumption of a 16-element rectangular antenna array at the receiver, positions of coherent sources are estimated in a wide sector of azimuth and elevation angles. The developed neural model does not require special preprocessing technique to decorrelate signals. Simulation results demonstrate the ability of the model to provide more accurate results than 2D MUSIC algorithm with spatial smoothing preprocessing technique. Besides, the RBF neural model is able to operate in real-time and outperforms MUSIC with SSP in terms of speed of computation.

## Acknowledgement

This work was supported by the project TR-32052 of the Serbian Ministry of Education, Science and Technological Development.

## References

- [1] Schmidt, R. (1986) Multiple emitter location and signal parameter estimation. *IEEE Transactions on Antennas and Propagation*, 34, 276–280.
- [2] Roy, R. & Kailath, T. (1989) Esprit-estimation of signal parameters via rotational invariance techniques. *IEEE Transactions on Acoustics, Speech, and Signal Processing*, 37, 984–995 .
- [3] Yi, H. & Zhou, X. (2005) “On 2-D Forward-Backward Spatial Smoothing for Azimuth and Elevation Estimation of Coherent Signals,” *antennas and propagation society international symposium*. In: *IEEE*, Vol. 2b, pp. 80–83.
- [4] Agatonovic, M., Stankovic, Z., Doncov, N., Sit, L., Milovanovic, B. & Zwick, T. (2012) Application of artificial neural networks for efficient high-resolution 2D DOA estimation. *Radioengineering*, 21, 1178–1186.